Processing, morphology and properties of a thermotropic liquid crystalline polymer

B. Zülle and A. Demarmels*
Asea Brown Boveri, Corporate Research CRBV, CH-5405 Baden-Dättwil, Switzerland

and C. J. G. Plummer and H.-H. Kausch
Laboratoire de Polymères, Ecole Polytechnique Fédérale de Lausanne, CH-1015 Lausanne, Switzerland
(Received 9 July 1992)

The relationship between processing parameters, morphology and properties has been investigated for injection mouldings and extrudates of filled and unfilled grades of a thermotropic copolyester. Low injection speeds were found to result in a significant increase in tensile strength and modulus in the flow direction. This was correlated with an increase in the thickness of the highly oriented skin layer and also with improved molecular orientation of the core regions. Tensile tests on single layers confirmed the skin to have a higher tensile strength and modulus than the core, and the tensile properties to correlate well with the local orientation. With the addition of mineral filler, the influence of injection speed on tensile properties became less marked, and the properties within the mouldings were more homogeneous. The adhesion between the layers also improved in the presence of filler. Additional tests were carried out on extruded tubes. The extensional flows associated with the extrusion process lead to relatively high molecular orientation in the extrusion direction and therefore to good mechanical properties.

(Keywords: liquid crystalline polymer; injection moulding; extrusion; morphology; orientation; mechanical properties)

INTRODUCTION

Commercial structural thermotropic liquid crystalline polymers (TLCPs) are linear-chain thermoplastics, whose melt state is characterized by a high degree of local molecular alignment. This has its origins in the relatively high chain rigidity (the molecules are often idealized as high aspect ratio rigid rods), and is generally associated with an exceptionally low melt viscosity, whence TLCPs are well suited to the filling of extremely thin-walled cavities by injection moulding. Given their low melt shrinkage and low coefficients of thermal expansion, TLCPs thus offer considerable advantages over more traditional materials in applications such as precision moulding. Other advantages of TLCPs include their excellent barrier properties, chemical resistance and temperature resistance[1-6].

In the present study however, we have been concerned with the potentially exceptional mechanical properties engendered by flow-induced macroscopic alignment of the rigid TLCP molecules during processing. This phenomenon has its analogue in the flow-induced alignment of glass or other fibres in short fibre reinforced thermoplastics, and has led to the frequent use of the term 'self-reinforcing polymers' when referring to TLCPs. The mechanical properties of TLCPs are thus typically highly anisotropic, and likely to be very much better in the flow direction than those of conventional thermoplastic resins, depending on the distribution and extent of molecular orientation. The latter are highly sensitive to the type of processing route, and the choice of processing parameters.

TLCP mouldings typically display layered morphologies, with the layers themselves often containing a striking hierarchy of fibrillar or sublayer structure[7-14]. Generally the outermost or 'skin' layers contain the highest degree of molecular orientation in injection mouldings, with the core orientation being much reduced, or in some cases even transverse to the melt flow direction[14-21]. Clearly the proportions of these different layers within the cross-section of an injection-moulded sample will play an important role in determining the overall mechanical properties. There has in consequence been considerable interest in the influence of injection parameters on the layer morphology of injection mouldings[12].

The proportions of the different layers in injection mouldings appear to be greatly influenced by heat transfer, the skin thickness being found to decrease with increasing mould temperature for example. The orientation of each layer depends strongly on the fluid dynamics of the mould filling process[22,23] and the improvement in mechanical properties at low injection speeds has also been linked by Duska[7] to reduced viscous heating between the skin and the core, and reduced melt viscosity at low injection pressures. Fillers were held by Duska to diminish the influence of the injection parameters because of their diluent effect and their raising of the thermal conductivity of the melt[7].

TLCPs are also suitable for extrusion in spite of their tendency to split (as a result of the fibrillar structure). Since the extensional flow fields associated with extrusion are more effective in inducing molecular orientation in

* To whom correspondence should be addressed

0032-3861/93/173628-10

Table 1 Materials

Grade	Filler	wt%
A950	None	–
A515	Wollastonite ($CaSiO_3$)	15
A540	Wollastonite ($CaSiO_3$)	40

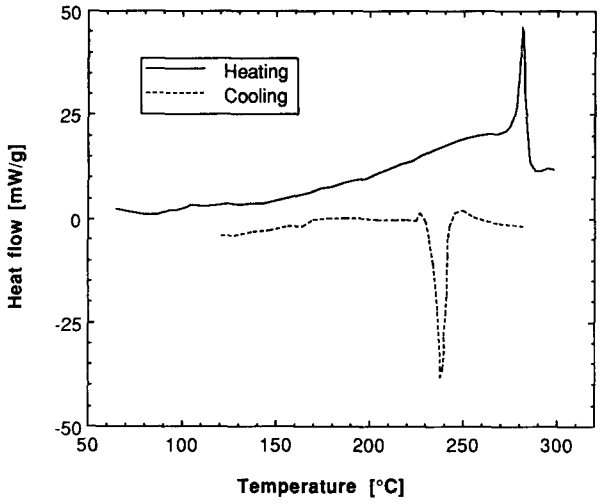

Figure 1 D.s.c. curves for the as-received A950 granulate; heating (second run) and cooling (scanning rate 20 K min^{-1})

TLCPs than shear flow[24], one might anticipate generally better mechanical properties in the flow direction than for injection mouldings, in which shear flow predominates. Indeed, relatively high moduli and tensile strengths have been reported for extruded TLCP rods in the literature[25–27]; with internal air cooling of the nozzle, a modulus of ~85 GPa has been measured for an 0.8 mm extruded TLCP rod[26,27], which is between three and four times greater than typical values for TLCP injection mouldings. The sample geometry and draw rate have an important influence on these mechanical properties. To promote uniformly high orientation throughout the sample, for example, draw ratios greater than two are required[28,29]. With counter-rotation of the core and the outer cylinder, biaxial orientation can also be induced which improves the shear modulus[30,31].

EXPERIMENTAL

Materials

A commercial thermotropic copolyester, Vectra™ (Hoechst Celanese), consisting of 27 mol% hydroxynaphthoic acid and 73 mol% hydroxybenzoic acid with different amounts of mineral filler was used (*Table 1*).

The thermal properties of these materials have been extensively discussed in the literature[32–35]. D.s.c. curves generally indicate a melting peak at ~280°C and a solidification peak on cooling at ~230°C (*Figure 1*). In order to exclude the influence of the processing of the granulate, the second heating run is shown. The transition energies (2–4 J g^{-1}) are much smaller than for conventional thermoplastics, this having been ascribed both to a lack of three-dimensional order in the solid state, and to the relatively small change in orientational order on solidification[33]. D.s.c. also reveals a second-order transition close to 100°C, and torsion pendulum measurements show a corresponding α peak, often referred to as the glass transition (*Figure 2*).

Sample preparation

Tensile specimens (4 mm × 10 mm cross-section) were injection moulded using a Battenfeld 650/400 injection moulding machine (screw diameter 45 mm, Unilog 4000 steering, open die) with different injection speeds and pressure limits. The influence of injection speed, holding pressure and screw rotation speed during feeding was also investigated for samples injected using a Netstal Cycap 60 injection moulding machine (shut-off die).

Tubes with various diameters and wall thicknesses were extruded with a Cincinnati extruder (BM screw, diameter 45 mm, length/diameter = 30, cylinder temperature 250°C — in fact the true melt temperature is likely to be higher than the nominal cylinder temperature owing to frictional heating). The outer and inner diameters of the ring die were 16 and 11 mm, respectively. The tube was cooled in a water bath and drawn-off at between 4.4 m min^{-1} and 5.8 m min^{-1}.

In all cases, the as-received granulate was dried either for a minimum of 4 h at 150°C (following the supplier's recommendations) or for 15 h at 110°C prior to moulding. This latter procedure had the advantage of minimizing bridging in the hopper of the processing machines.

Characterization

The samples were sectioned with a diamond saw and the layer dimensions were measured from the corresponding colour variations as observed using reflected light optical microscopy. The orientation of individual layers machined from the mouldings was determined using wide-angle X-ray scattering (WAXS, Siemens D500, Cu $K\alpha_1$ radiation) and that of microtomed samples from i.r. dichroism measurements (Mattson Sirius 100 FT-IR spectrometer). The tensile tests were performed with a Schenck hydropuls PSA40 at a crosshead speed of 2 mm min^{-1}. Scanning electron microscopy (SEM) was used to examine fracture surfaces, and the surfaces of layers delaminated during fracture.

RESULTS AND DISCUSSION

Injection mouldings

Tensile fracture surfaces. Both the filled and unfilled injection mouldings (*Figure 3*) show a clear skin–core

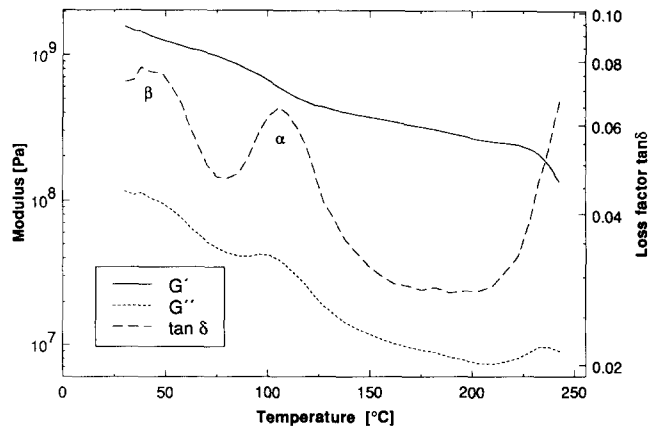

Figure 2 Torsional pendulum test for a compression-moulded A515 sample

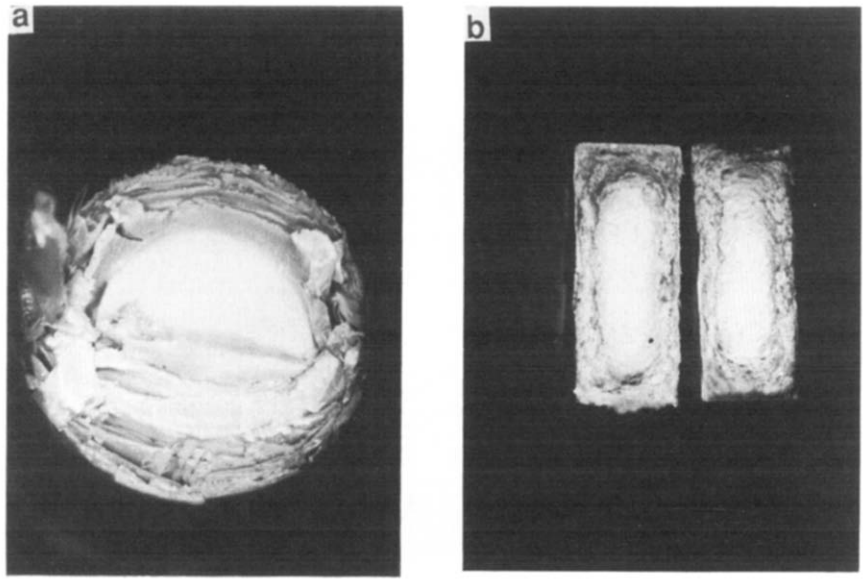

Figure 3 Section of (a) the sprue of an unfilled moulding and (b) the tensile fracture surface of a 40 wt% mineral filled moulding

morphology, with a marked sublayer structure. During fracture of the unfilled mouldings there is widespread delamination of these layers, and the core is often drawn out of the remainder of the sample over distances of several centimetres, and in extreme cases over the whole gauge length. At 15 wt% filler content however, the separation of the points of skin and core failure along the samples is substantially reduced (1–2 cm), and at 40 wt% filler content delamination is often negligible (*Figure 4*). Where there is delamination, the core has a tendency to break close to the shoulder regions furthest from the gate. This is possibly because the orientation and the strength are reduced by the locally diverging flow in such regions (*Figure 5*) and because the far wall of the mould disturbs the flow. Morphological investigations presented elsewhere point both to highly chaotic flow away from the gate, as well as a tendency for local transverse orientation to develop in association with 'flow lines' within the core, which may represent points of local weakness. The skin, on the other hand, appears to show more uniform properties along the length of the sample.

From the decrease in the separation of the points of failure of the skin and core with increasing filler content, it might also be inferred that adhesion between the different layers improves with filler content. This is also suggested by SEM observations (*Figure 6*). The surfaces between the layers of the unfilled mouldings are relatively smooth, with little interconnecting material. Indeed, regions of delamination are also encountered in the inner regions of the unfilled mouldings. *Figure 6b* shows part of the fracture surface of a sample from which a 0.5 mm layer had been machined from the surface prior to testing. For the mineral filled grades, it may be seen from *Figure 6a* that the delamination surfaces of the skin layers are rougher than in the case of the unfilled material, with a considerable amount of fibrillar structure connecting skin and core. Such observations might also be taken to imply a lower degree of molecular orientation along the axis of the filled mouldings.

Tensile tests; the effect of moulding conditions. The effect of injection rate, holding pressure and rotation speed of the screw during feeding on the properties of the 4 mm × 10 mm cross-section tensile specimens has been systematically investigated for mouldings in which the mean melt temperature and mould temperature were maintained at 280 and 80°C, respectively. On the basis of observations using SEM and light optical microscopy, three different types of morphology were distinguished, depending on the fill rate, as shown in *Table 2*. The relationship of these to injection rates and tensile strengths is shown in *Figure 7* for the unfilled grade. Broadly, 'type 2' morphologies, found at high injection rates ($> 30\ cm^3\ s^{-1}$) are distinguished by a relatively large outer core region and tensile strengths and Young's moduli of the order of 110 MPa and 6 GPa, respectively, for the unfilled grade, and 120 MPa and 12 GPa for the 40 wt% wollastonite filled grade. In 'type 1' morphologies, corresponding to moderate injection rates ($10–30\ cm^3\ s^{-1}$), the extent of the intermediate layer and skin is increased at the expense of the outer core, and there are modest increases in tensile strength and moduli for both unfilled and filled grades. Finally, for the unfilled grade at lower injection rates, 'type 3' morphologies dominate, with a smaller, 'layered' core, and a somewhat higher proportion of skin, leading to tensile strengths and moduli as high as 220 MPa and 12 GPa, respectively.

Although the proportion of skin is also increased, it is not possible to distinguish clear 'type 3' morphologies at low injection speeds for 40 wt% filler (for which there is, in any case, a much less clear demarcation of the different structural regions). The corresponding increase in tensile strength is weaker, with maximum values not exceeding 140 MPa. The modulus, on the other hand, may reach 21 GPa for fill rates of $5\ cm^3\ s^{-1}$.

A higher feed rate (screw rotation speed) leads to improved preorientation of the melt, which is probably maintained to some extent in the finished moulding. Increasing the time during which the hold pressure is maintained also appears beneficial, possibly since it prevents back flow of the melt (*Figure 8*).

Measurements on individual layers. In order to measure the mechanical properties in different regions of

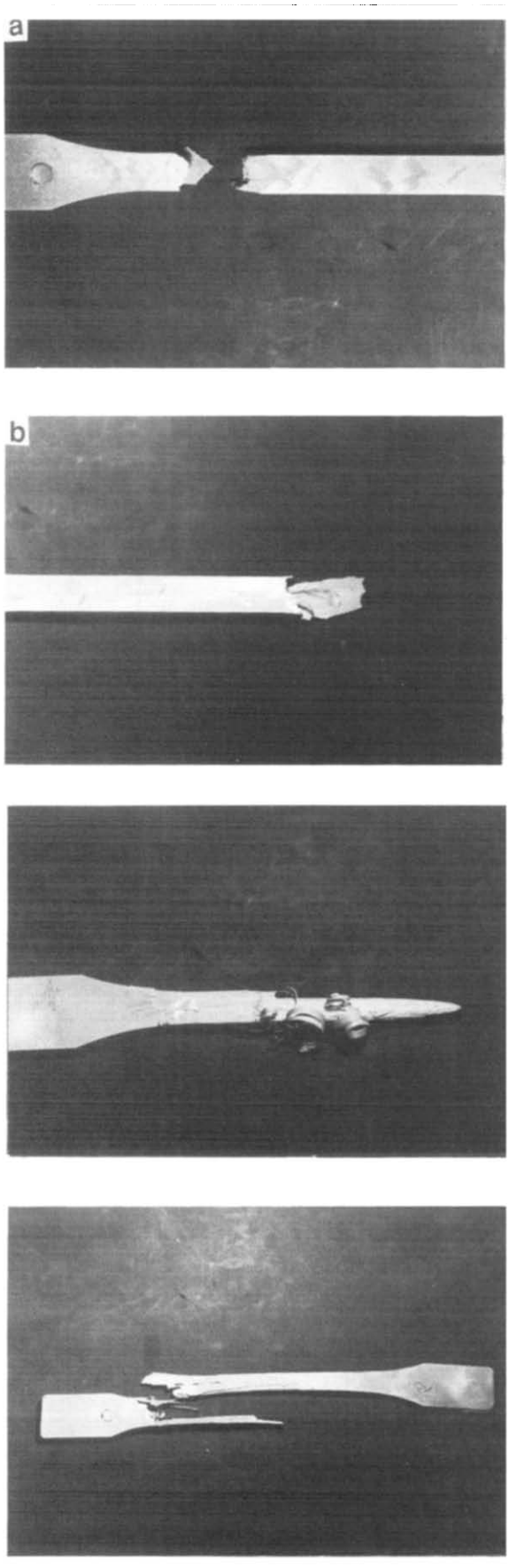

Figure 4 (a) Fracture surface of a 40 wt% mineral filled moulding (23°C, crosshead speed 2 mm min^{-1}). The flow direction during mould filling is from right to left. (b) Fracture surfaces of unfilled 4 mm × 10 mm mouldings. The upper two parts belong to the same specimen. From the lower specimen, a 0.5 mm layer had been machined from the surface prior to testing (23°C, crosshead speed 2 mm min^{-1}). The flow direction during mould filling is from right to left

the samples, parts of tensile bars were removed by machining, so that only one layer carried the load during the test. The resolution of this method is somewhat limited owing to handling problems with samples whose thickness is $<300\,\mu m$. Typical results are illustrated in *Figures 9–11*. The skin regions in unfilled samples are characterized by high strengths and low extensions to fail compared to the intermediate layers, but the extensions to fail are similar to those of the whole mouldings, suggesting that skin fracture determines the overall strength of the latter. This implies further that the contribution to overall strength from the inner layers is dependent on their stiffness at the failure strain, rather than their strength.

At low injection speeds the strain to fail of the core is higher than that of the skin, whilst at high injection speeds the situation is reversed. One reason for this may be the changes in the shear rate profiles within the mould. In reference 36 it has been demonstrated using the Moldflow computer simulation package, that at high injection speeds the shear rate maximum is close to the sample walls, promoting plug flow of the central regions. At low injection speeds however, the shear maximum moves towards the interior of the sample. This may lead not only to improved orientation of the inner layers, but also to disruption of the flow-line structure referred to earlier, which may develop earlier in the melt history (e.g. at the gate).

Addition of filler leads to a progressive decrease in the differences between the strengths and high strain stiffness of the different layers. Thus whilst in the unfilled mouldings the load is concentrated in the skin at failure, at 40 wt% filler content, it is more evenly distributed over the sample cross-section. Thus where the proportion of skin is low, for example, in a moulding with a relatively large total cross-section, the strength of the unfilled mouldings may well fall below that of the filled mouldings. Indeed, for unfilled 4 mm × 10 mm mouldings with relatively low tensile strengths, the inner regions often continue to bear loads up to and beyond the load at which the skin fails.

Since failure of whole unfilled samples is observed to be initiated by failure of the skin layers, it is assumed that to a first approximation, the overall tensile strength, σ_{tot}, is given by:

$$\sigma_{tot} = \sum_l \sigma_l(\varepsilon_f)\alpha_l \qquad (1)$$

where $\sigma_l(\varepsilon_f)$ is the stress in each layer l at the failure strain, and α_l is the area proportion of each layer in the sample cross-section. Some examples for this calculation are given in *Table 3*.

On the basis of stress–strain measurements, it was found that differences in properties between the fast and slow unfilled injection mouldings are dominated by the increase in the proportion of the skin, but that there is

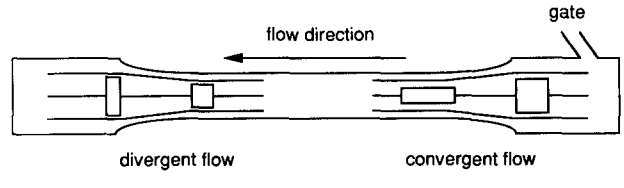

Figure 5 Schematic diagram of melt flow during injection moulding

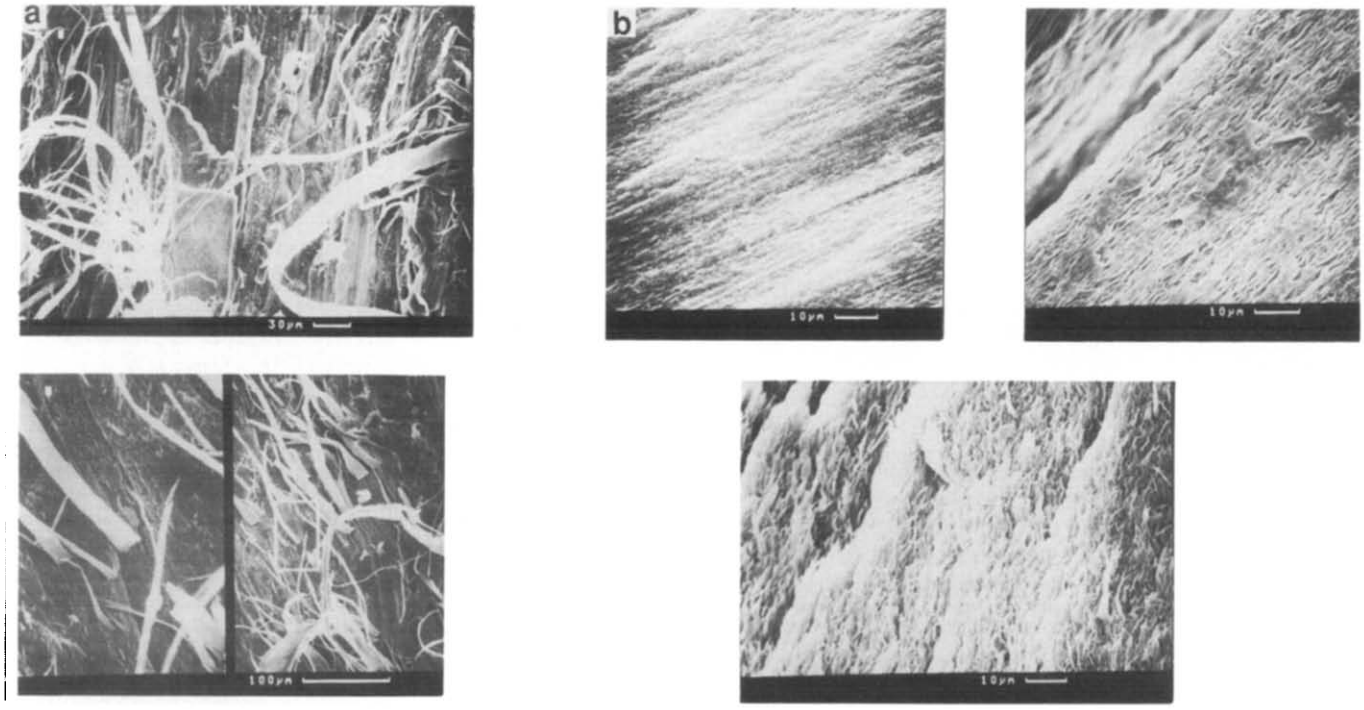

Figure 6 (a) SEM micrographs of delamination of the skin layer, and the core fracture surface in a 40 wt% mineral filled moulding (23°C, 2 mm min^{-1}). (b) SEM micrographs of delamination of different layers during tensile fracture of an unfilled moulding (23°C, 2 mm min^{-1})

Table 2 Sample morphologies in injection mouldings of Vectra

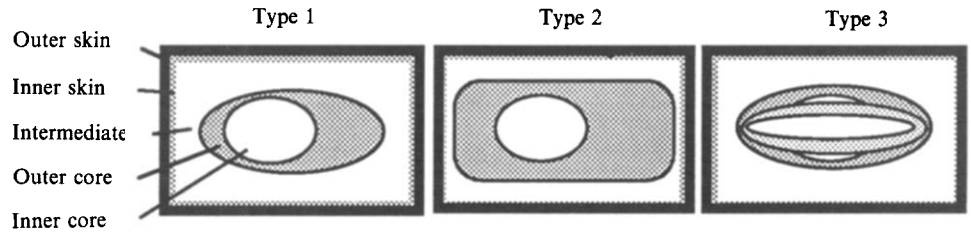

Region	% of cross-section		
Outer and inner skin	10–20	5–10	20–30
Intermediate	50–60	20–30	50–60
Outer core	10–20	50–60	10–20
Inner core	10–20	10–25	2–8

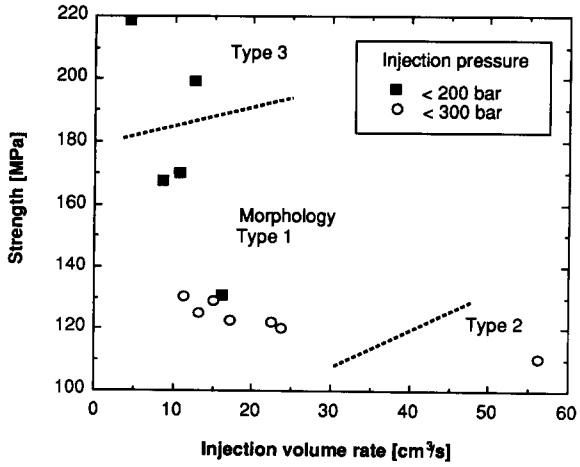

Figure 7 Influence of injection parameters on the tensile strength of unfilled mouldings injected with the Battenfeld machine (23°C, 2 mm min^{-1})

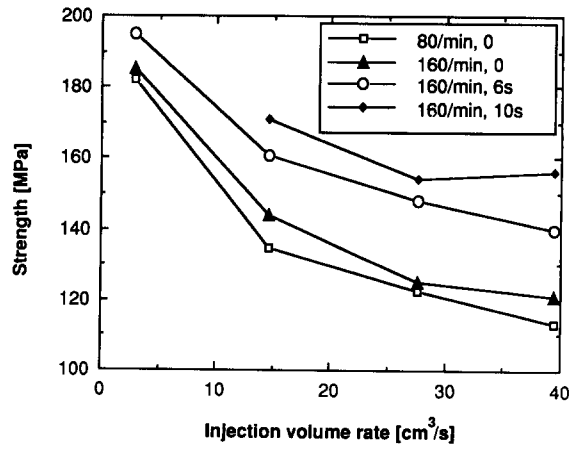

Figure 8 Influence of moulding conditions on tensile strengths in 15 wt% mineral filled mouldings (injected with the Netstal machine). The screw rotation speed and the duration of holding pressure are indicated

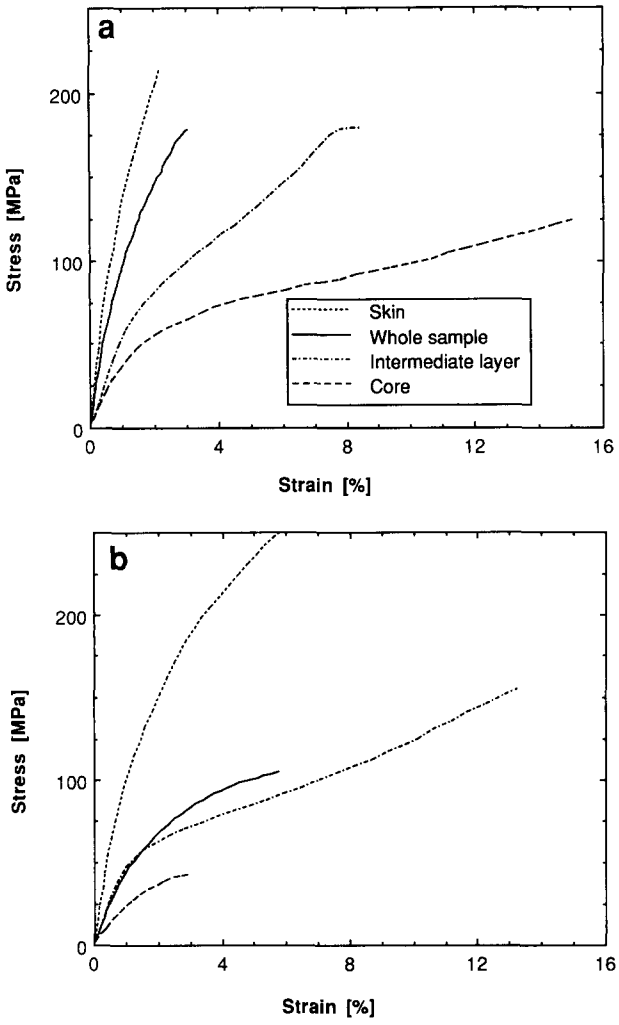

Figure 9 Stress–strain curves for layers from unfilled mouldings. Injection speed: (a) 5; (b) 40 $cm^3 s^{-1}$ (23°C, 2 mm min^{-1})

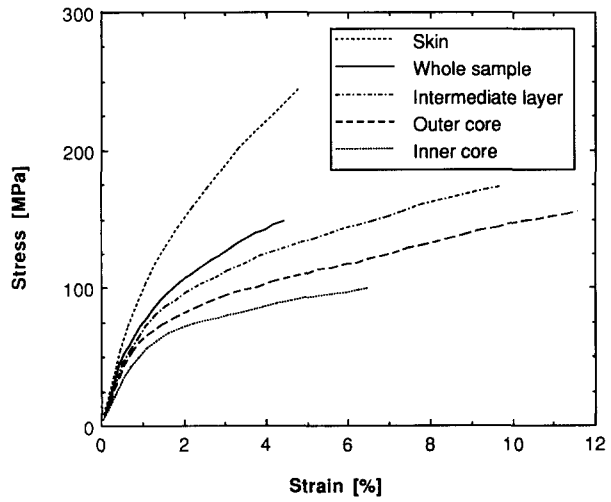

Figure 10 Stress–strain curves for layers from 15 wt% mineral filled mouldings (23°C, 2 mm min^{-1})

a significant contribution from stiffening of the inner regions at high strains.

There is also evidence in the literature that simple mixing rules based on the proportion of skin may account for the variations in properties with fill rate (through the changes in the skin proportion)[23]. In view of the role of changes in the inner layers, this may be an over-simplification in the present case. Nevertheless, as *Figure 12* shows, it is possible to establish a correlation between mechanical properties and skin thickness, with data for samples produced under various moulding conditions.

It has also been found that stopping mould filling just before the melt front reaches the far end of the sample, leads to increases in tensile strength even though there are no variations in skin thickness. These increases are due to increases in the stiffness of the inner layers (such that they are bearing more load at the point of skin failure), possibly as a result of elimination of backflow effects[8].

The higher strength and modulus of samples with a higher skin proportion suggests that one might improve the properties by using, for example, I-beam type cross-sections as opposed to solid sections, which would also save on materials costs and weight. This has been investigated by using detachable inserts in the pre-existing moulds, as illustrated in *Figure 13* for 4 mm × 10 mm dumb-bell specimens. [Since the resulting mouldings were not necessarily symmetric, the filled grades (here 15 wt% wollastonite) were used in order to minimize warping.] Intrinsic values for the room temperature Young's modulus and tensile strength for fixed moulding conditions for a variety of cross-sections are plotted against the effective wall thickness of the mould. Substantial increases in modulus are seen as the wall thickness decreases, such that the effective modulus

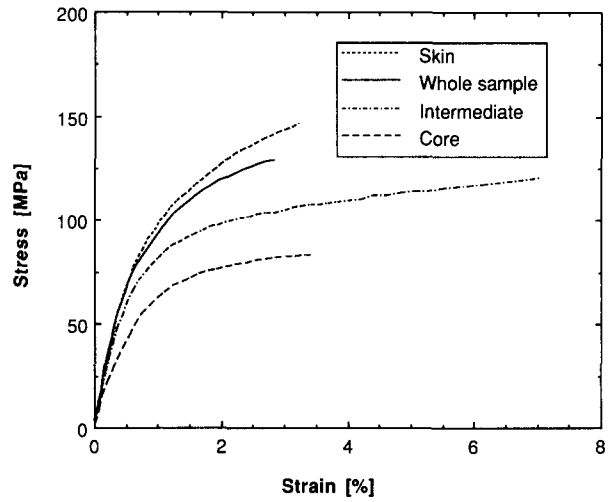

Figure 11 Stress–strain curves for layers from 40 wt% mineral filled mouldings (23°C, 2 mm min^{-1})

Table 3 Comparison of the strength (in MPa) calculated on the basis of measurements on single layers with the experimental strength of whole samples

	Unfilled slow inj.	Unfilled fast inj.	15 wt% mineral
Skin (%)	25	12	20
$\sigma_f(\varepsilon_f)$	250	250	250
Int. layer (%)	65	63	50
$\sigma_f(\varepsilon_f)$	120	90	130
Core (%)	10	25	30
$\sigma_f(\varepsilon_f)$	75	45	100
Calc. strength	148	99	145
Expt. strength	170	105	160

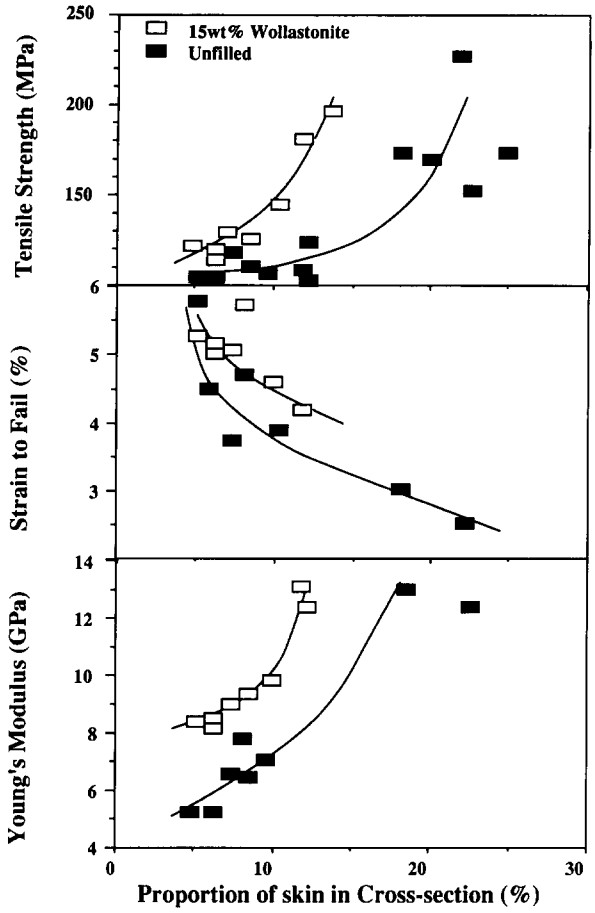

Figure 12 Correlation between skin proportion and tensile properties in unfilled and in 15 wt% mineral filled mouldings (23°C, 2 mm min^{-1})

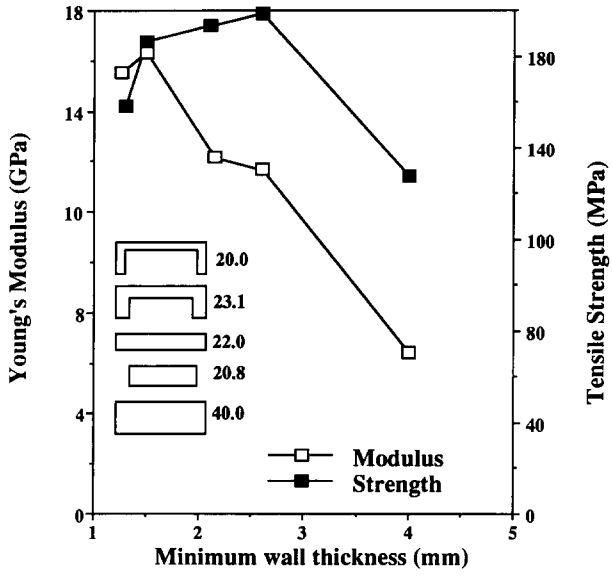

Figure 13 Effect of different sample cross-sections on the tensile properties of 15 wt% mineral filled mouldings (23°C, 2 mm min^{-1}). The cross-sections and cross-sectional areas (in mm^2) are given in increasing order of minimum wall thickness

(normalized with respect to the cross-sectional area of the standard 4 mm × 10 mm sample) is raised by up to 50% even though the cross-section contains 50% less material. The strength does not increase indefinitely, since at small wall thicknesses, large changes in effective mould cross-section close to the sample ends resulted in weak points at the ends opposite the gate, where there are locally strong diverging flows.

Orientation distributions. The use of WAXS methods for the measurement of molecular orientation of TLCPs is well documented in the literature. It involves measurement of the height of the main scattering peak as a function of the sample orientation direction, which in turn gives information on the angular distribution of the molecular orientation[17], described by the Hermans orientation function, S, given by:

$$S = 0.5\langle 3\cos^2\theta - 1\rangle \quad (2)$$

where θ is the angle between the long axis of individual molecules and the preferred orientation direction, and the angular brackets represent a global average taken over all the molecules present.

This is not the only method. I.r. dichroism measurements have been used[20,21], although here the information is less quantitative unless detailed information is available regarding possible differences between the orientation of the principal axes of the optical indicatrix and the chain direction. In view of this uncertainty, X-ray measurements provide a more reliable measure of molecular orientation, and have been preferred here.

In an X-ray diffraction vector scan, two main peaks are observed: $2\theta = 19.5$, which corresponds to the interchain distance of 4.5 Å and $2\theta = 44$, which corresponds to the intrachain distance of 2.1 Å (*Figure 14*)[17].

According to Mitchell and Windle[17], the orientation function S can be calculated from the intensity measured as a function of the sample orientation α around the X-ray beam with the scattering vector **s** fixed at $2\theta = 19.5$:

$$S = -2\frac{\int_0^{\pi/2} I(\mathbf{s},\alpha)\frac{1}{2}(3\cos^2\alpha - 1)\sin\alpha\, d\alpha}{\int_0^{\pi/2} I(\mathbf{s},\alpha)\sin\alpha\, d\alpha} \quad (3)$$

In general WAXS measurements of S as defined by equation (3), such as shown for layer samples in *Figure 15* taken from the 4 mm × 10 mm mouldings, indicate an increase in orientation in the outer layers of the samples. *Figure 16* also suggests a tendency for wollastonite addition to lower the difference in orientation between the skin and the core. Further,

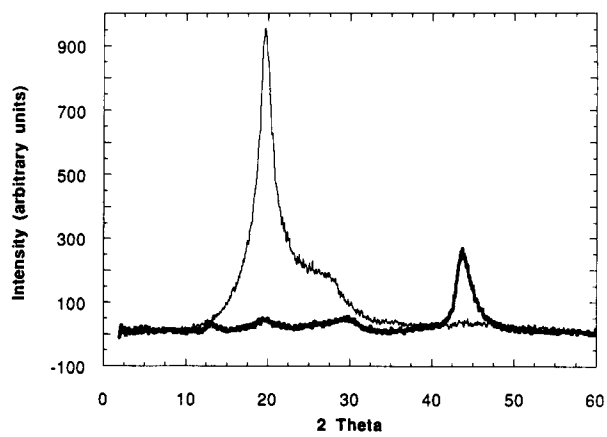

Figure 14 X-ray measurement for a skin layer from an unfilled moulding, $\alpha = 0$ (thick line) and $\alpha = \pi/2$ (thin line). α is the angle of rotation of the sample

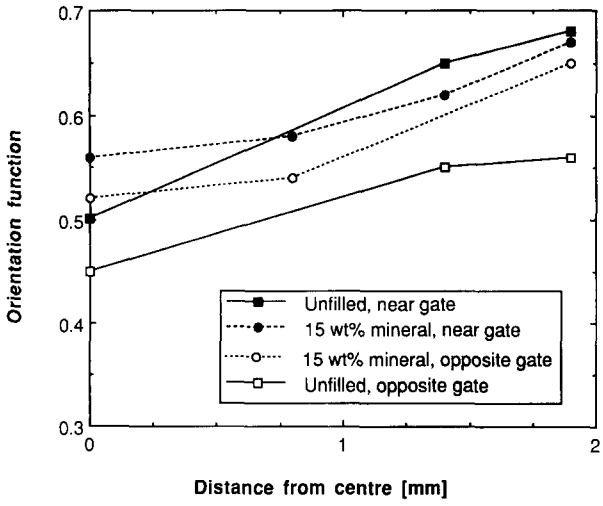

Figure 15 Orientation in regions near and opposite the gate measured at different points in the sample cross-section for the 4 mm × 10 mm mouldings

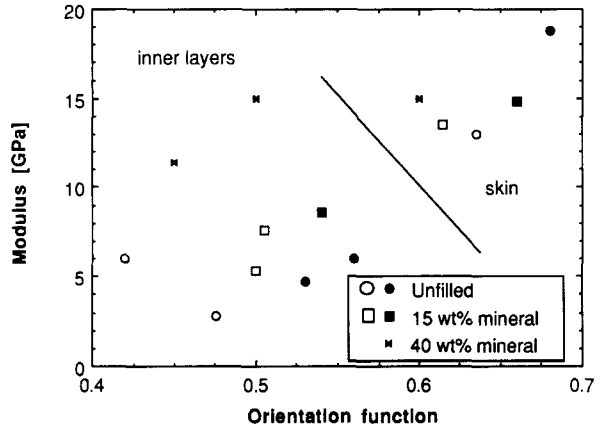

Figure 16 Effect of filler addition on Young's modulus for a given matrix orientation. The different symbols refer to layers obtained from samples moulded with different injection velocities: (open symbols) 40 $cm^3 s^{-1}$; (filled symbols) 5 $cm^3 s^{-1}$; (×) 20 $cm^3 s^{-1}$ (23°C, 2 mm min^{-1})

whereas a substantial drop in S is observed close to the shoulder region opposite the gate in the unfilled samples, this is less marked on addition of filler.

Layers with low orientation often have relatively large strains to fail. In such cases, the orientation after the tensile test is significantly higher. As with the modulus, results for the 15 wt% filled material lie between those for the unfilled and the 40 wt% filled grades (*Figure 17*).

Extrusion

Extruded tubes of unfilled and 15 wt% mineral filled Vectra have been tested in tension and compression at room temperature and 80°C. The tube diameter was between 7 mm and 16 mm and the wall thickness between 1 mm and 3 mm. The different dimensions were obtained by varying the draw ratio and supporting air pressure. Two methods have been used to clamp the specimens in the testing machine (*Figure 18*): the ends of the tubes were encased in epoxy. Transverse steel pins were employed to prevent the tube from slipping out of the epoxy block; and a steel pin was glued lengthways along the inside of the tube before direct clamping. In some cases, the sample was wrapped in sandpaper to minimize damage from the grips.

Microscopic investigation of cross-sections showed a skin–core morphology as in injection-moulded parts (*Figure 19*). The links which maintain the inner part of the extrusion die in position result in longitudinal knit lines in the tubes.

Thin sections have been taken from the skin, the intermediate and the core regions, both at and away from the knit lines, in order to measure the orientation function by X-ray diffraction as described in the previous section. The orientation in association with the knit lines is considerably diminished in the unfilled samples (*Table 4*). The mineral filled tubes are more homogeneous however, and in fact the orientation in the knit line regions is often improved in the presence of filler. In both the unfilled and the filled samples, higher draw down ratios lead to higher orientation.

Values for the moduli of the tubes are shown in *Table 5*. As it was impossible to fix the extensometer to the very short (1 cm) specimens used for measuring the compression strength, long samples (as for tensile tests) were compressed by 1 mm to determine the modulus. For comparison, values of a tube of polyester mat reinforced epoxy are also given. The TLCP tubes are much stiffer at room temperature, and comparison with the results in references 25–27 shows that with higher draw down ratios, even higher values of orientation and modulus are potentially obtainable.

The compressional strength at room temperature is ~100 MPa (compared with 120 MPa for the polyester/epoxy tube) and at 80°C, ~40 MPa (compared with 65 MPa for the polyester/epoxy tube). None of the samples broke within the gauge length, so that the experimental values for the tensile strength are lower limits. These nevertheless compare well with the strengths obtained for the injection-moulded samples.

CONCLUSIONS

The morphology and properties of injection-moulded TLCPs are strongly dependent on several parameters, which may in turn be interdependent. Some aspects of this are shown in *Figure 20*. Lower injection speeds lead to higher shear forces because of the cooling of the melt and so to higher orientation of the inner layers and to a

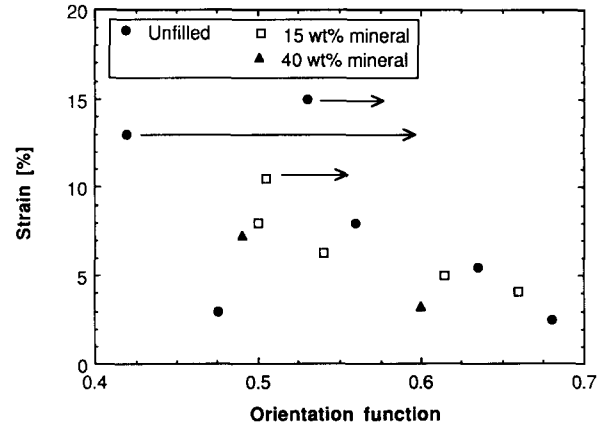

Figure 17 Strain to fail for layers from filled and unfilled mouldings. The arrows indicate changes in orientation as measured subsequent to the tensile tests (23°C, 2 mm min^{-1})

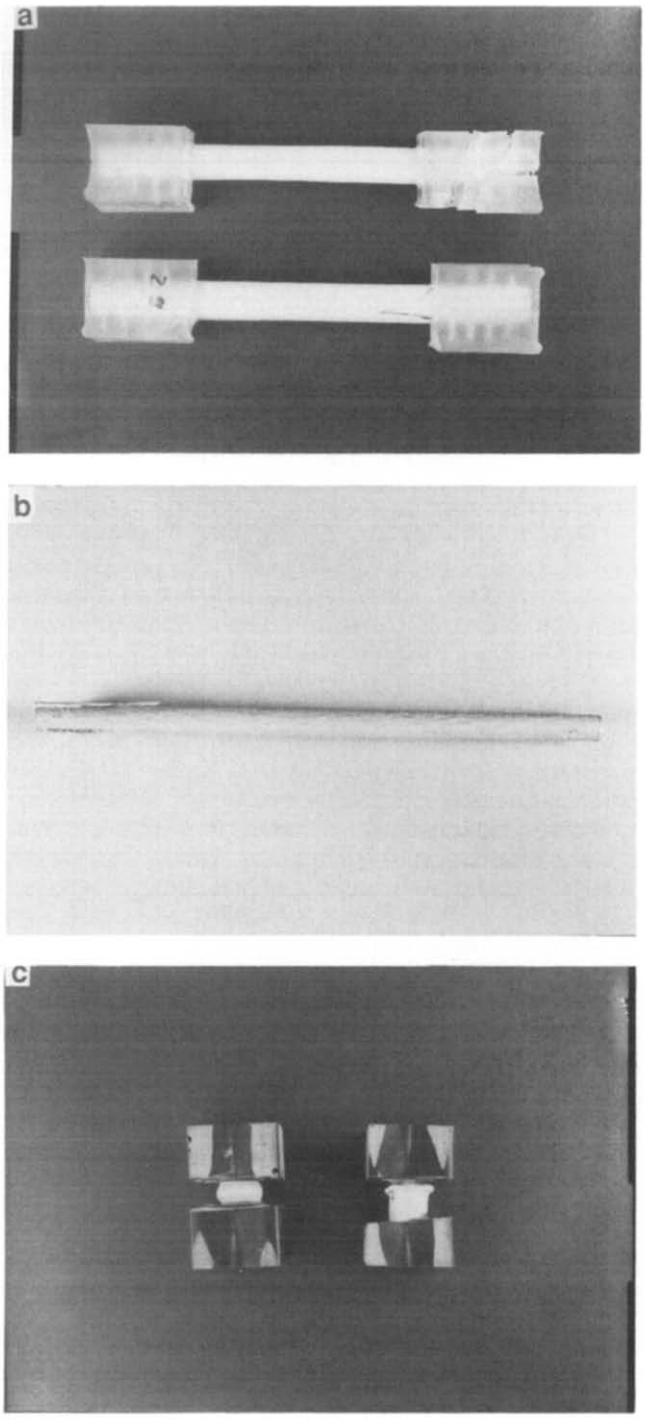

Figure 18 Specimens for (a, b) tensile and (c) compression tests. The ends of the samples (a) and (c) are protected by epoxy. Tube diameter: (a) 16; (b) 7; (c) 16 mm

thicker skin. Therefore, tensile strength and modulus are increased in the axial direction. The proportion of skin can also be increased by a comb-like shape of the cross-section. The prior melt history (delay time in the cylinder, rotation speed of the screw) influences also the morphology and the final properties. Extrusion leads both to high levels of orientation and to a more homogeneous orientation distribution than in injection mouldings, resulting in relatively good mechanical properties in the axial direction.

Particle addition tends to reduce orientation to some extent, but particle filled sampls nevertheless retain a high degree of anisotropy. Perhaps a more significant effect of filler addition is that it tends to even fluctuations in orientation, both within a given cross-section and in the flow direction. In unfilled samples, high orientation differences between skin and core lead to stress concentrations in the skin, which is relatively stiff. Thus, even if the skin strength is high, overall failure (which initiates in the skin) may occur at relatively low loads.

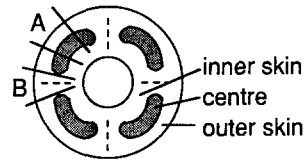

The 4 knit lines (sector B) are caused by the 4 links in the die

Figure 19 Schematic diagram of the cross-section of an extruded tube

Table 4 Values of the orientation function for extruded tubes of unfilled and mineral filled TLCP

		Inner skin		Centre		Outer skin	
	λ	A[a]	B[a]	A	B	A	B
Unfilled	1	0.58	0.55	0.63	0.50	0.64	0.50
	2	0.64	0.62	0.68	0.66	0.71	0.68
15 wt% wollastonite	1	0.56	0.56	0.53	0.58	0.60	0.57
	2	0.57	0.60	0.65	0.66	0.66	0.65

[a] A and B indicate the position within the cross-section with reference to *Figure 19*

Table 5 Tensile and compression modulus (in GPa) for TLCP and polyester mat/epoxy tubes[a]

		Tension		Compression	
	λ	23°C	80°C	23°C	80°C
Unfilled	1	10	5	12	5
	2	14	9	17	9
15 wt% wollastonite	1	11	7.5	15	9
	2	18	12	18	10.5
Polyester/epoxy		5.5	4.3	6.7	4.4

[a] As the TLCP samples are not perfectly circular in cross-section, there is an error in the cross-sectional area and consequently in the modulus of ~10%

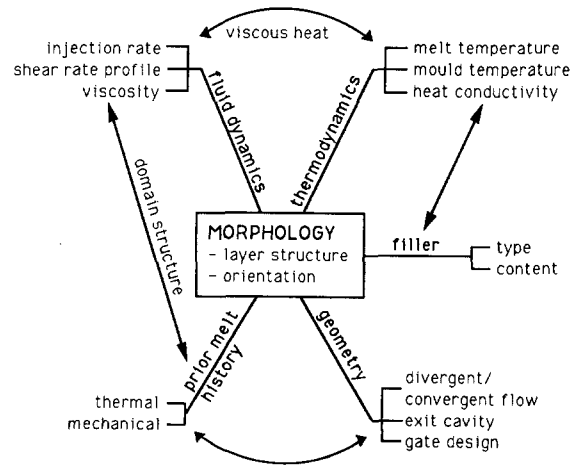

Figure 20 Aspects of morphology formation of injection-moulded TLCP

With fillers, there is better load distribution within the sample cross-section, owing both to lower orientation variations and also the fact that the high strain behaviour of the stress–strain curves is very similar, in spite of orientation variations, owing to the contribution of debonding to the shape of the former. Thus whilst optimized moulding conditions may lead to higher tensile strengths for unfilled samples, owing to the fact that particle addition will lower the tensile strength for a given orientation, filled grades will tend to perform better where moulding conditions are not optimized (the effect of filler on the tensile strength is in practice small, but for 40 wt% filled grades the room temperature strength will probably not exceed ~140 MPa). This allows more flexibility in mould design and turnover rates, where tensile strength is an important consideration. In particular, it allows exploitation of the possibility offered by TLCPs of fast cycle times — to obtain the best performance from unfilled TLCPs low fill rates are required. This is quite apart from the other advantages of filler addition, and in particular of a systematic increase in modulus in the flow direction with filler content.

ACKNOWLEDGEMENTS

The authors wish to thank Professor W. Kaiser and M. Diez, HTL Brugg-Windisch, and Huber & Suhner Ltd, Herisau, for their help with the injection moulding and extrusion, and Professor P. Brüesch for helpful suggestions regarding the orientation measurements. Financial support from the Swiss Commission pour l'Encouragement de la Recherche Scientifique (CERS) is gratefully acknowledged.

REFERENCES

1 Carfagna, C., Amendola, E., Mensitieri, G. and Nicolais, L. *J. Mater. Sci. Lett.* 1990, **9**, 1280
2 Chiou, J. S. and Paul, D. R. *J. Polym. Sci., Polym. Phys. Edn* 1987, **25**, 1699
3 Weinkauf, D. H. and Paul, D. R. *J. Polym. Sci., Polym. Phys. Edn* 1991, **29**, 329
4 Brostow, W. *Kunststoffe* 1988, **78**, 411
5 Collyer, A. A. *Mater. Sci. Technol.* 1989, **5**, 309
6 Cox, M. K. *Rapra Rev. Reports* 1987, **1**
7 Duska, J. J. *Plast. Eng.* 1986, **42**, 39
8 Boldizar, A. *Plast. Rubber Proc. Appl.* 1988, **10**, 73
9 Kenig, S. *Polym. Comp.* 1986, **7**, 50
10 Menges, G., Schacht, T., Becker, H. and Ott, S. *Int. Polym. Proc.* 1987, **2**, 77
11 Ophir, Z. and Ide, Y. *Polym. Eng. Sci.* 1983, **23**, 792
12 Suokas, E. *Polymer* 1989, **30**, 1105
13 Sawyer, L. C. and Jaffe, M. *J. Mater. Sci.* 1986, **21**, 1897
14 Weng, T., Hiltener, A. and Baer, E. *J. Mater. Sci.* 1986, **21**, 744
15 Economy, J., Volksen, W. and Geiss, R. H. *Mol. Cryst. Liq. Cryst.* 1984, **105**, 289
16 Mitchell, G. R., Windle, A. H. *Polymer* 1983, **24**, 1513
17 Mitchell, G. R. and Windle, A. H. *Dev. Cryst. Polym.* 1988, **2**, 115
18 Ide, Y. and Ophir, Z. *Polym. Eng. Sci.* 1983, **23**, 261
19 Joseph, E. G., Wilkes, G. L. and Baird, D. G. *Polym. Eng. Sci.* 1985, **25**, 377
20 Pirnia, A. and Sung, C. S. P. *Macromolecules* 1988, **21**, 2699
21 Barres, O., Friedrich, C., Jasse, B. and Noel, C. *Makromol. Chem., Macromol. Symp.* 1991, **52**, 161
22 Williams, G. E. and Garg, S. K. *Japan-US Polym. Symp. Prepr.* 1985, 39
23 Kenig, S., Trattner, B. and Andermann, H. *Polym. Comp.* 1988, **9**, 20
24 Baird, D. G., Joseph, E., Pissipati, R., Viola, G. and Wilkes, G. L. 'Proc. 42nd Ann. Techn. Conf. Soc. Plast. Eng.', New Orleans, 1984, p. 508
25 Chen, J. C., Gorky, D. V., Haley, R. C., Jaarsma, F. C. and McChesney. 'Techn. Papers, Reg. Techn. Conf.', 1985, p. 61
26 Chung, T. S. *J. Polym. Sci., Polym. Lett. Edn* 1986, **24**, 299
27 Chung, T. S. *J. Polym. Sci., Polym. Phys. Edn* 1988, **26**, 1549
28 Jenkins, J. C. and Jenkins, G. M. *J. Mater. Sci.* 1987, **22**, 3784
29 Kenig, S. *Polym. Eng. Sci.* 1989, **29**, 1136
30 Farell, G. W. and Fellers, J. F. *Polym. Eng. Rev.* 1986, **6**, 263
31 Michaeli, W., Ott, S., Meier, M., Brinkmann, T. and Heidemeyer, P. *Synthetic* 1990, **10**, 42
32 Blundell, D. J. *Polymer* 1982, **23**, 359
33 Blundell, D. J., Macdonald, W. A. and Chivers, R. A. *High Perf. Polym.* 1989, **1**, 97
34 Bechtoldt, H., Wendorff, J. H. and Zimmermann, H. J. *Makromol. Chem.* 1987, **188**, 1015
35 Sarlin, J. and Törmälä, P. *J. Polym. Sci., Polym. Phys. Edn* 1991, **29**, 395
36 Diez, M., Bader, C. and Kaiser, W. *Kunststoffe* 1991, **81**, 705